

# EROSION-OXIDATION OF PRESSURE VESSEL STEEL P265GH

E. HUTTUNEN-SAARIVIRTA<sup>1\*</sup>, V.-T. KUOKKALA<sup>1</sup>, M. ANTONOV<sup>2</sup>, R. VEINTHAL<sup>2</sup>, J. TUIREMO<sup>3</sup>, K. MÄKELÄ<sup>3</sup>

<sup>1</sup> Department of Materials Science, Tampere University of Technology, P.O. Box 589, FI-33101 Tampere, Finland.

<sup>2</sup> Department of Materials Engineering, Tallinn University of Technology, Ehitajate tee 5, 19086 Tallinn, Estonia

<sup>3</sup> Metso Power Oy, Lentokentänkatu 11, P.O. Box 109, 33101 Tampere, Finland

## ABSTRACT

The behaviour of pressure vessel steel P265GH was studied in a centrifugal high-temperature erosion apparatus under impacts by silica (SiO<sub>2</sub>) particles moving at velocities ranging from 20 to 60 m s<sup>-1</sup> and contacting the surface at the angles of 30° and 90°. Besides particle impacts, the steel was simultaneously exposed to air and elevated temperatures of 350 and 450°C. For comparison, the tests were also performed in the absence of erodent particles. After the tests, the material behaviour was evaluated in terms of occurred weight changes and surface characteristics, the latter ones of which were investigated by using, for example, scanning electron microscopy (SEM) and energy-dispersive X-ray spectroscopy (EDS). In the analysis of the test results, special attention was paid to the composition and microstructure of the used silica particles and how these influence the elemental distribution on the exposed surfaces. The results show that the particle impacts introduce weight losses that follow a ductile angle-dependency, i.e., relatively greater weight losses at the shallow than at the steep impact angle. Although evident oxide scales developed on the surfaces at the test temperatures, they did not provide the steel with protection against particle impacts. Particle debris was detected embedded in the surfaces particularly under impacts at 90°, with softer particle constituents being preferentially deposited. These results are discussed in terms of the erosion-oxidation behaviour of the steel and the consequences of the heterogeneous erodent particle quality.

Keywords: Erosion-oxidation, erosion, oxidation, particle, steel

\* Corresponding author: Elina Huttunen-Saarivirta ([elina.huttunen-saarivirta@tut.fi](mailto:elina.huttunen-saarivirta@tut.fi)).

## INTRODUCTION

Erosion-oxidation of alloys occurs in elevated-temperature processes, such as fluidized-bed combustion, where erosive wear due to impacts by moving solid particles and elevated-temperature oxidation due to oxidizing atmosphere occur simultaneously and compete. The relative intensities of the two phenomena determine the combined action and the overall rate of degradation; under some conditions, oxidation may

enhance the rate of erosion damage, while under other conditions, oxidation may provide protection against particle impacts [1].

All variables that influence the interactions of the erodent particles and the prevailing atmosphere with the alloy also affect its erosion-oxidation behaviour. Understanding on how several key variables, such as impact angle and velocity of the erodent particles as well as temperature, influence the mechanism and rate of erosion-oxidation of several alloys

has been achieved as a result of extensive research. The area which has gained much less attention is the characteristics of the erodent particles and their role in erosion-oxidation [2]. Although a consensus has been reached that angular and large SiO<sub>2</sub> particles generally cause more wastage than spherical and small particles containing significant amounts of Ca and S [3-6] there are some evident gaps in the knowledge in this area. For example, the research by Levy and Man [4] showed that erosion-oxidation wastage of 9Cr1Mo steel at 650°C is significantly higher by using “red” SiO<sub>2</sub> than “white” SiO<sub>2</sub>, although the sands had nominally the same composition and equal properties, such as hardness. The difference in the erosivity was attributed to different sharpness of the protrusions on the particles, although such difference was not visually evidenced. Indeed, it is challenging to precisely characterize the erodent particles that in all cases exhibit some variation in size, shape, composition and properties and that are used in significant amounts. However, it is evident that more research effort in this area is needed.

In this study, erosion-oxidation of pressure vessel steel P265GH, which is often used as a heat exchanger material in fluidized-bed boilers, was studied at the temperatures of 350 and 450°C under a range of particle impact conditions. Further, special attention was paid to the compositional and microstructural heterogeneity of the used SiO<sub>2</sub> particles and how these are linked to the behaviour of the particles and the steel in the erosion-oxidation tests.

## EXPERIMENTAL PROCEDURES

A pressure vessel steel P265GH (according to EN standard), containing 0.149 wt% C, 0.92 % Mn and 0.20 % Si, was used as a test alloy. It was in a roll normalized condition and had

a ferritic-pearlitic microstructure, an average grain size of 19 µm and a hardness of 137 HV. The steel was obtained as plates of 4 mm in thickness, of which the specimens of 23 x 12 mm were cut. For the tests, the specimens were ground to 600 grit surface finish and cleaned using acetone and ethanol. The erodent in erosion-oxidation tests was silica (SiO<sub>2</sub>) sand that is used as a bed material in an operating fluidized-bed combustion (FBC) unit.

Erosion-oxidation tests were carried out at 350 and 450°C using a four-channel centrifugal high-temperature erosion apparatus described in detail elsewhere [7]. For each test, 6 kg of fresh silica sand was used. In the tests, the particles moved at the velocities of 20, 40 and 60 m s<sup>-1</sup> and contacted the specimens at the angles of 30 and 90°. For comparison, the tests were also performed in the absence of erodent particles; in these oxidation tests, the apparatus was operated as for the erosion-oxidation tests at 20 m s<sup>-1</sup>. The duration of each test was determined by the consumption of the loaded sand, being typically some tens of minutes.

The size distribution of the particles was determined by a laser diffraction method using a Sympatec Helos H9093 device. The shape, morphology and composition of the particles as well as the elemental distribution and micro-hardness in their cross sections were determined using a Philips XL30 scanning electron microscope (SEM), equipped with an EDAX energy dispersive spectrometer (EDS) and an Anton Paar µ-Indenter 5 microhardness tester. The phase structure of the particles was analyzed using a Siemens D-500 X-ray diffractometer and CuK<sub>α</sub> radiation. Hardness of the sand particles was also measured using Buehler Omnimet hardness measuring system and the load of 300 g. Weighing of the steel specimens was carried out to an accuracy of 0.1 mg before and after the erosion-oxidation

and oxidation tests, enabling the average specimen weight changes to be determined. Surfaces of the exposed specimens were examined using a Philips XL30 SEM. Hardness of the steel was determined using a Struers Duramin A-300 hardness measuring equipment and the load of 3 kg.

## RESULTS

### Erodent particles

The as-received particles were characterized in terms of size, shape, composition, phase structure, elemental distribution and microhardness. The mean size of the particles was 398  $\mu\text{m}$ , with more than 80% of the particles falling in the range from 200 to 600  $\mu\text{m}$ . SEM studies of the particles (Fig. 1a) revealed evident roundness together with some occasional sharp edges, enabling the particle shape to be characterized as slightly angular. SEM examinations also showed that the particles had a relatively irregular surface morphology. EDS analyses yielded an average particle composition of 61.7 % O, 30.4 % Si, 4.4 % Al, 1.1 % K, 0.8 % Na, 0.7 % Fe, 0.7 % Mg and 0.2 % Ca. A cross-sectional study of the particles disclosed compositional heterogeneity (Fig. 1b). Majority of the particles contained mainly Si and O, and these particles were characterized by microhardness values in the range from 872 to 1084 HV. These particles were seldom fragmented in specimen preparation. The remaining minority of the particles contained Al, K, Mg and O, plus occasionally some Fe. These particles were often fragmented during specimen preparation and showed microhardness values in the range from 610 to 775 HV. XRD analyses indicated the particles to be structurally heterogeneous: several XRD spectra were measured and all were slightly different. However, in each case, the major phases that were detected were quartz,  $\text{SiO}_2$ , and orthoclase,

$\text{Al}_2\text{O}_3 \cdot \text{K}_2\text{O} \cdot 6\text{SiO}_2$ , the variation in the spectra being due to the changes in their relative amounts and texture. The average hardness of the sand was 1183 HV.

### Erosion-oxidation and oxidation tests

Fig. 2 shows weight changes for the steel tested under impacts by sand particles and, for comparison, in the absence of particles, at 350°C (Fig. 2a) and 450°C (Fig. 2b). At both temperatures, particle impacts caused weight losses, i.e., weight gains smaller than in oxidation tests or true weight losses, while weight gains were obtained in oxidation tests. In the absence of particles, slightly higher weight gains were detected at 450°C than at 350°C (the ratio of detected weight gains was 2:1), consistent with oxidation rates increasing with increase in temperature. As for the results from erosion-oxidation tests, there was a trend for the amount of wear losses to increase with increase in temperature, particularly at an angle of 90°. At both test temperatures, the magnitude of weight losses increased also with increase in particle velocity. Furthermore, under all test conditions, weight losses were greater at an angle of 30° than at 90°.

### Exposed surfaces

SEM examinations of the surfaces exposed to air in the absence of sand particles revealed evident oxide scales and their spallation at both temperatures (Figs. 3a-b). According to XRD, the oxide scales were magnetite, i.e.,  $\text{Fe}_3\text{O}_4$ . The corresponding studies of the surfaces exposed to the particles disclosed differences in the morphology and composition between the studied impact conditions, particularly between the impact velocities and angles. At an angle of 30° at the lowest velocity (Fig. 4a), cutting type of deformation was detected, primarily in the steel but also in the oxide scales that covered some areas. The deformation tracks were

relatively small and shallow. Hence, oxide scales were occasionally detected on the steel, particularly at 450°C, whereas at the higher impact velocities or at an angle of 90°, such scales were evidently less frequent. Particle debris was often detected embedded in the surface. At the highest velocity (Fig. 4b), there was clearly more evidence of cutting type of deformation than at the lower velocities, the extent and depth of individual deformation tracks being greater than at the lower velocities. This manifests greater wear rate at higher particle velocities. Furthermore, the areas where particle debris was embedded in the surfaces were essentially more abundant than at the lower velocities.

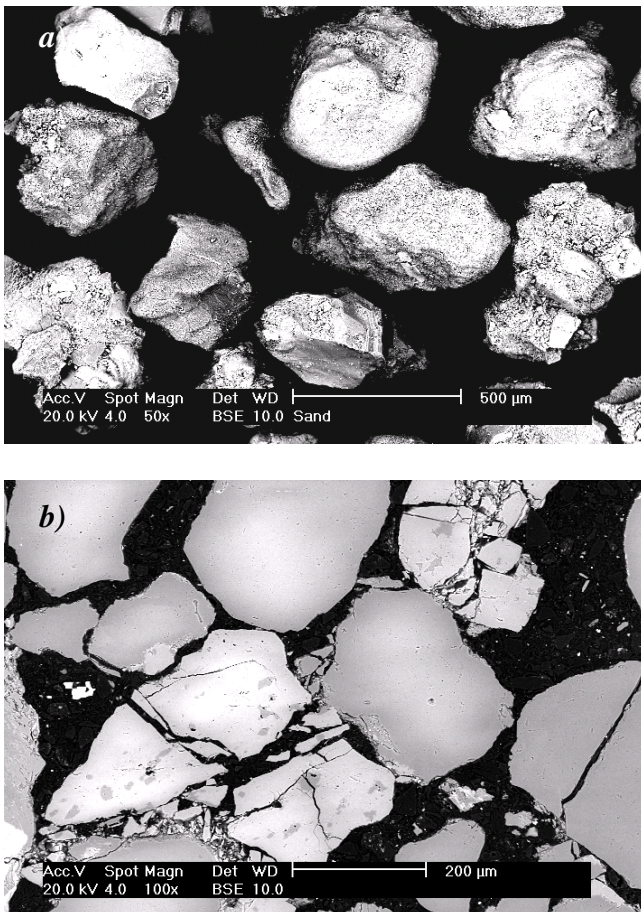


Figure 1. BSE SEM image of erodent particles. a) Surface. b) Cross-section.

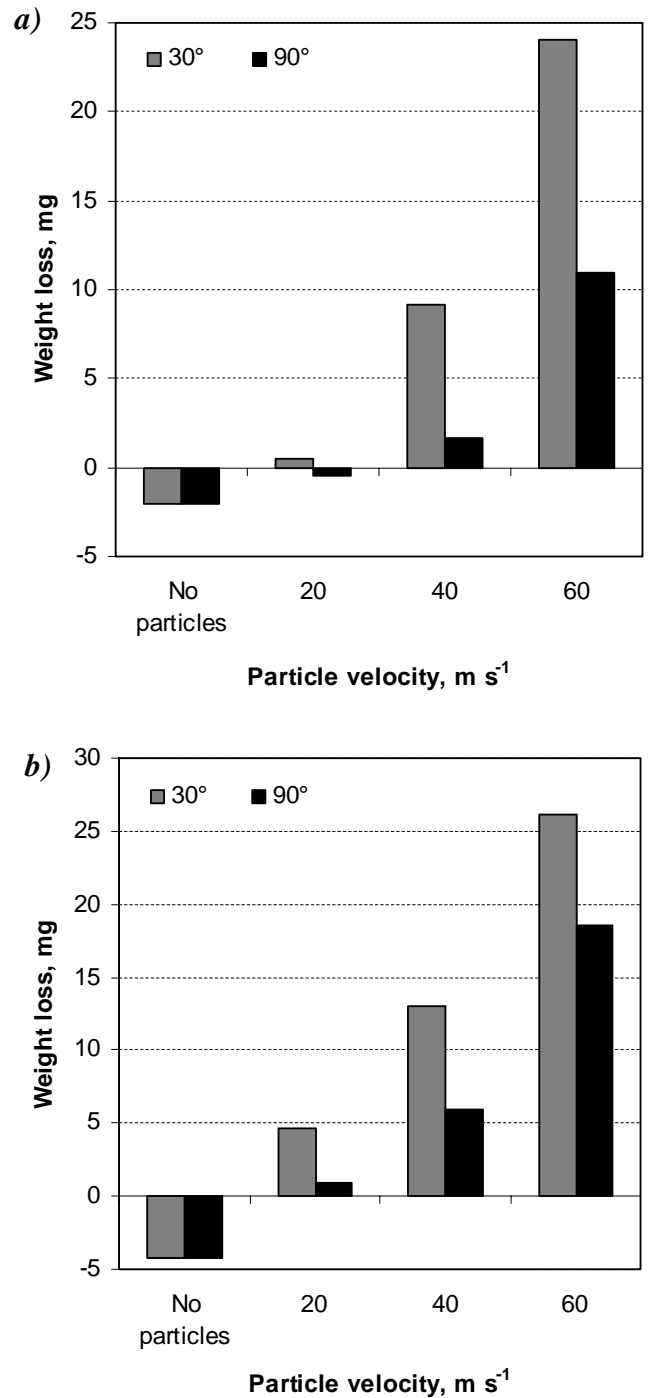


Figure 2. Weight changes for the steel under several conditions at a) 350° and b) 450°C.

At an angle of  $90^\circ$  at the lowest velocity (Fig. 5a), impact craters could be detected on the surfaces, although these were relatively shallow. Much of the surface was covered by deposited particle debris. However, oxide scales were not evident on the surfaces. At the highest velocity (Fig. 5b), the most pronounced surface feature was the formation of impact craters, the number and depth of which were essentially greater than at the lowest velocity, indicating higher erosion rate. Some particle debris was detected on the surface, primarily at the rims of the craters.

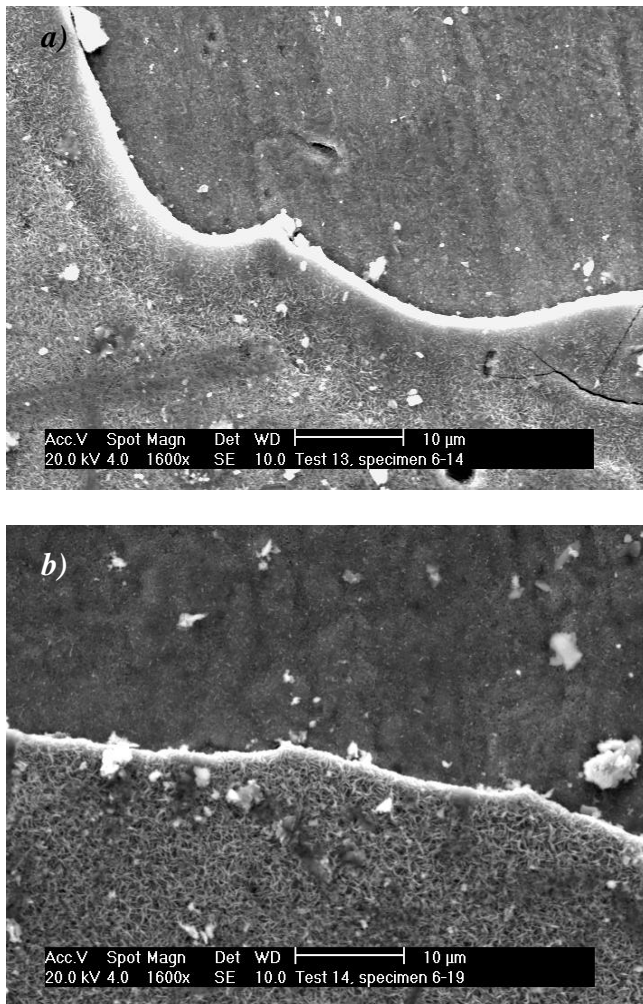


Figure 3. SEM image of the surface exposed in absence of the erodent particles. a)  $350^\circ\text{C}$ . b)  $450^\circ\text{C}$ .

Between the two test temperatures, the differences in the morphology of surfaces exposed to sand particles were minor. The only dissimilarity that could be detected was the extent of oxidation of the steel, as evaluated on the basis of EDS analyses obtained in such areas where the steel was not covered by particle debris. Not surprisingly, slightly more oxidation was detected at  $450^\circ\text{C}$  than at  $350^\circ\text{C}$ .

The observation that the worn surfaces contained significant amounts of particle debris that also showed some compositional variation triggered an investigation whether there exists a correlation between the particle impact conditions and the amount or type of elements detected on the damaged surfaces. Such investigation was conducted by determining the share of various erodent elements, primarily silicon, aluminum and potassium, on the exposed surfaces by using several EDS analyses and neglecting the share of oxygen and the elements included in the steel. Fig. 6 shows the determined shares of the erodent elements under various test conditions, revealing two apparent trends. First, the share of the erodent elements in the surfaces exposed at an angle of  $90^\circ$  was significantly higher than that at  $30^\circ$ , irrespective of the test temperature. Second, there were some obvious differences between the share of the erodent elements in the damaged surfaces and the particle impact velocities. At an angle of  $30^\circ$ , the share of the erodent elements in the surfaces increased with increase in velocity from  $20$  to  $40\text{ m s}^{-1}$  and then slightly decreased with further increase in velocity at both temperatures. At an angle of  $90^\circ$  at  $350^\circ\text{C}$ , the share of the erodent elements in the damaged surfaces decreased with increase in particle velocity, while at  $450^\circ\text{C}$ , the lowest share of the erodent elements was detected at the intermediate velocity.

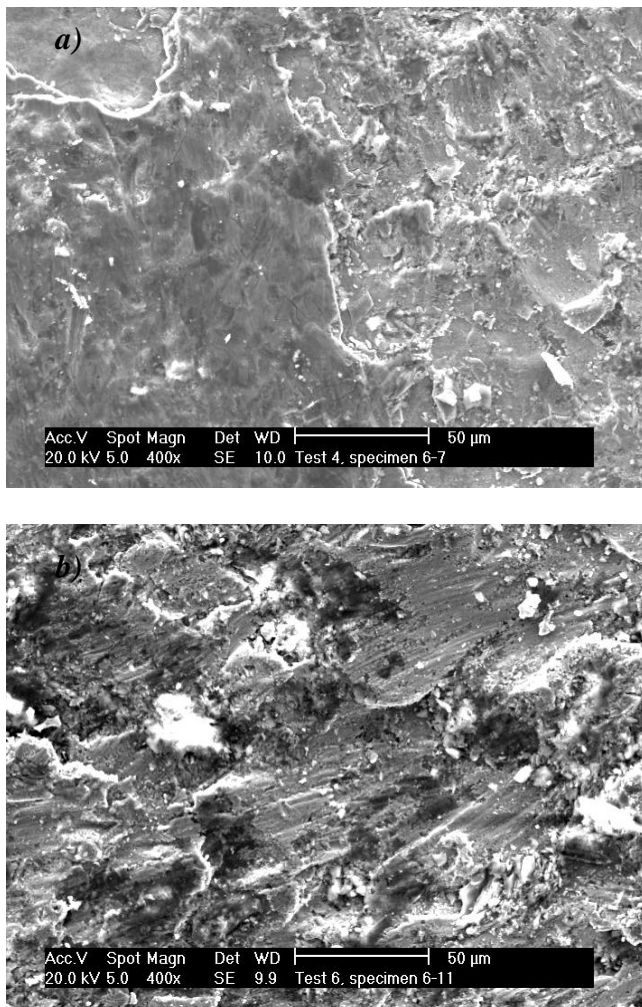


Figure 4. SEM image of the surface exposed at an angle of  $30^\circ$  at  $450^\circ\text{C}$ . a)  $20\text{ m s}^{-1}$ , b)  $60\text{ m s}^{-1}$ .

Compositional analyses disclosed that the share of aluminum in the damaged surfaces (in the range from 0.16 to 0.24) was essentially higher and that of silicon somewhat lower (in the range from 0.59 to 0.75) than in the as-received erodent (0.11 and 0.79, respectively), indicating that aluminum-containing parts of the particles showed greater tendency to be embedded in the damaged surfaces than silicon-containing parts. The analyses also showed that the surfaces impacted at  $30^\circ$  contained systematically slightly more aluminium than those impacted at  $90^\circ$ . At an angle of  $30^\circ$  at

the lowest velocities, the share of aluminum was highest, more than double as compared to that in the as-received erodent, but it slightly decreased with increase in velocity. In turn, the surfaces subjected to  $90^\circ$  impacts contained more silicon than those impacted at  $30^\circ$ , with no apparent differences being detected in the share of potassium between the damaged surfaces (in the range from 0.04 to 0.05) and the as-received erodent (0.03). It is emphasized that the low tendency of potassium in the particles to be deposited on the steel surfaces is a positive issue, since in waste- and biofuelled boilers, i.e., in the presence of chlorine, it could produce corrosive KCl deposits.

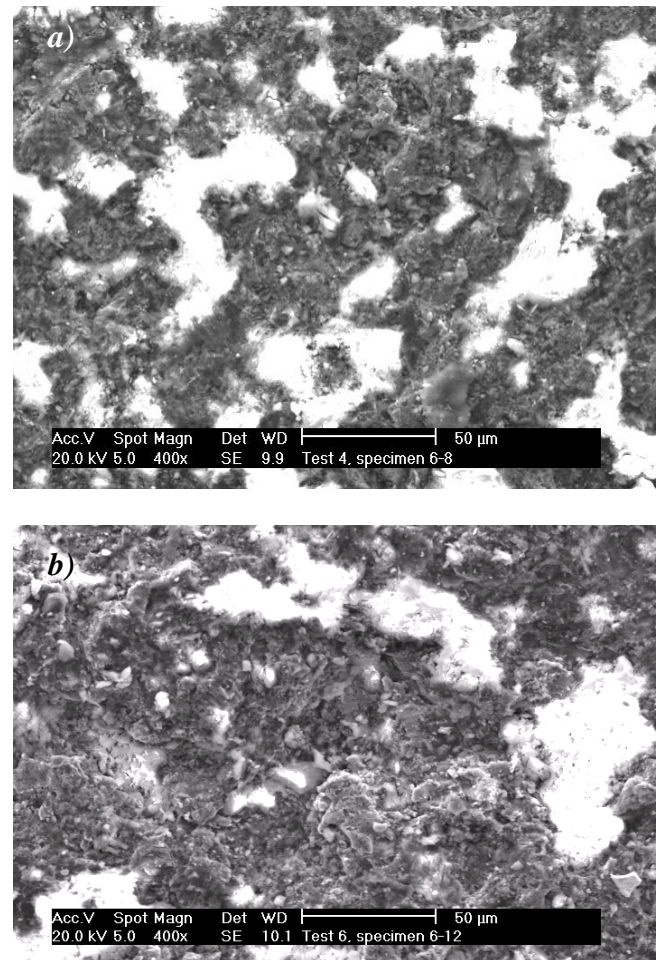


Figure 5. SEM images of the surface exposed at an angle of  $90^\circ$  at  $450^\circ\text{C}$ . a)  $20\text{ m s}^{-1}$ , b)  $60\text{ m s}^{-1}$ .

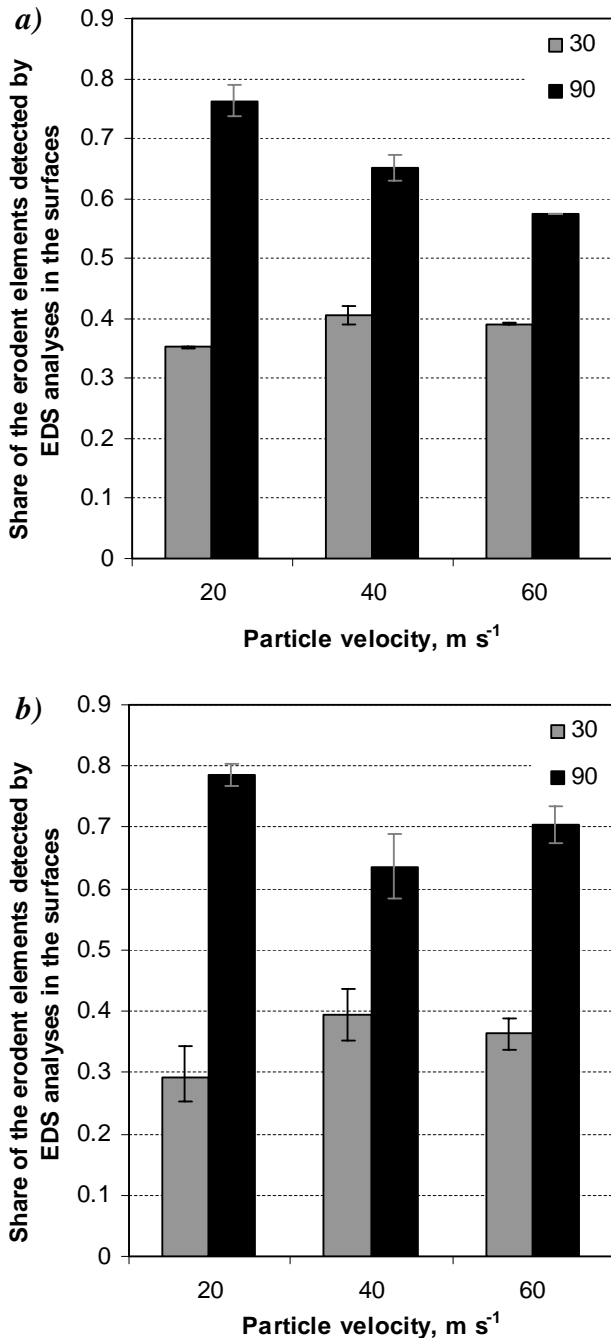


Figure 6. Share of the erodent elements in the surfaces exposed under several conditions at a) 350 °, b) 450 °C.

## DISCUSSION

The results from erosion-oxidation tests revealed that the studied steel showed a ductile erosion response, i.e., greater weight losses at a shallow than at a steep impact angle. At an angle of 30°, material removal occurred primarily by cutting and ploughing, with the relatively soft aluminum-containing parts of the sand particles being simultaneously embedded in the deformation track. Nevertheless, there was clearly more deposition of the sand particle debris in the exposed surfaces at 90°, thus compensating some of the material losses that occurred at this angle. Here, the wastage occurred through extrusion and, at higher velocities, probable cracking, as indicated by (steep) impact craters on the exposed surfaces. Further, the oxide scales, which are typically relatively more brittle than the underlying steel, were seemingly removed from the surfaces at 90°. The particles were more heavily fragmented in the normal impacts than at 30°, as manifested by the abundance of the particle debris and, particularly, silicon-containing parts of particle debris.

Under all test conditions, the weight losses for the steel increased with increase in particle velocity, evidently due to greater impact energies. In the worn surfaces, the greater wear rates were reflected to the higher frequency and volume of wear features: tracks or craters. However, there were slight differences in how the particles behaved during impact at the two angles with increase in velocity. At an angle of 30°, higher particle velocities introduced slightly more particle debris deposition in the exposed surfaces, with not only aluminum-bearing soft sections but also some of the silicon-containing particle bodies being retained on wear scars.

In turn, at an angle of 90°, the particles moving at higher velocities were probably more efficiently fragmented in the impact, leaving behind smaller debris of the particles than at the lower velocities.

The higher test temperature, 450°C, introduced thicker oxide scales than the lower temperature, 350°C. However, the scales were evidently brittle and did not provide the steel with protection against particle impacts. Instead, these were typically removed by particle impacts, which explains greater weight losses of the steel in erosion-oxidation tests performed at 450°C than at 350°C. Hence, the results suggest that for the studied steel, oxidation enhances the rate of erosion damage under all studied conditions. Such interaction between erosion and oxidation processes is typically termed oxidation-affected erosion [1].

Some previous studies [5] have suggested that deposition of soft particle constituents may form a continuous and protective layer on the exposed surfaces. In this study, the exposed surfaces contained a composite layer of deformed steel, oxide scale and embedded particle debris rather than a continuous layer of soft particle remnants. Further, we did not observe any evidence of the composite layer providing the steel with protection against further particle impacts. This is probably due to the fact that despite the local microhardness variations within the particles, the overall microhardness values of the erodent particles were much higher than those of the steel.

## CONCLUSIONS

- Pressure vessel steel P265GH shows a ductile erosion behaviour, i.e., greater weight losses at a shallow than at a steep impact angle. However, more deposition of the sand particle debris occurs when the particles contact the steel surfaces at

an angle of 90° than at 30°, thus compensating some of the wear losses that take place at a normal impact angle.

- For the studied steel, oxidation enhances the rate of erosion under all studied test conditions.
- The used sand particles are heterogeneous in terms of composition, microstructure and micro-hardness, with the aluminum-containing parts (orthoclase) being softer than pure silicon-bearing (quartz) parts. The heterogeneity of the particles influences their fragmentation on impact and, thus, the tendency to be embedded in the surfaces.

## ACKNOWLEDGEMENTS

The Academy of Finland is thanked for the funding for E.H.-S. (decisions 106160 and 218296). The Estonian Ministry of Education and Research (targeted finance projects SF0140091s08 and SF0140062s08) and Estonian Science Foundation (grant no. 8850) are acknowledged for the financial support to M.A. and R.V.

## REFERENCES

1. M.M. Stack, S. Lekatos, F.H. Stott, Erosion-corrosion regimes: number, nomenclature and justification? *Tribology International* 28, 1995, 445-451.
2. M.M. Stack, F.H. Stott, G.C. Wood, Review of mechanisms of erosion-corrosion of alloys at elevated temperatures. *Wear* 162-164, 1993, 706-712.
3. S.L. Palasamudram, S. Bahadur, Particle characterization for angularity and the effects of particle size and angularity on erosion in a fluidized bed environment. *Wear* 203-204, 1997, 455-463.



4. A.V. Levy, Y.-F. Man, Effect of particle variables on the erosion-corrosion of 9Cr1Mo steel. *Wear* 131, 1989, 53-69.
5. B.A. Lindsley, A.R. Marder, J.J. Lewnard, The effect of circulating fluidized bed particle characteristics on erosion of 1020 carbon steel. *Wear* 188, 1995, 33-39.
6. B. Wang, G. Geng, A.V. Levy, Erosivity of particles from operating fluidized bed combustors. *Wear* 150, 1991, 107-124.
7. E. Huttunen-Saarivirta, M. Antonov, R. Veinthal, J. Tuiremo, K. Mäkelä, P. Siitonen, Influence of particle impact conditions and temperature on erosion-oxidation of steel at elevated temperatures. *Wear* 272, 2011, 159-175.